A. T. Krause, S. Zschoche, M. Rohn, C. Hempel, A. Richter, D. Appelhans, B. Voit

Swelling behavior of bisensitive interpenetrating polymer networks for microfluidic applications

Erstveröffentlichung in / First published in:
Soft Matter. 2016, 12(25), S. 5529--5536 [Zugriff am: 04.11.2019]. Royal Society of Chemistry. ISSN 1744-6848.

DOI: https://doi.org/10.1039/c6sm00720a

Volume 12 | Number 25 | 7 July 2016 | Pages 5493–5654

Soft Matter

www.softmatter.org

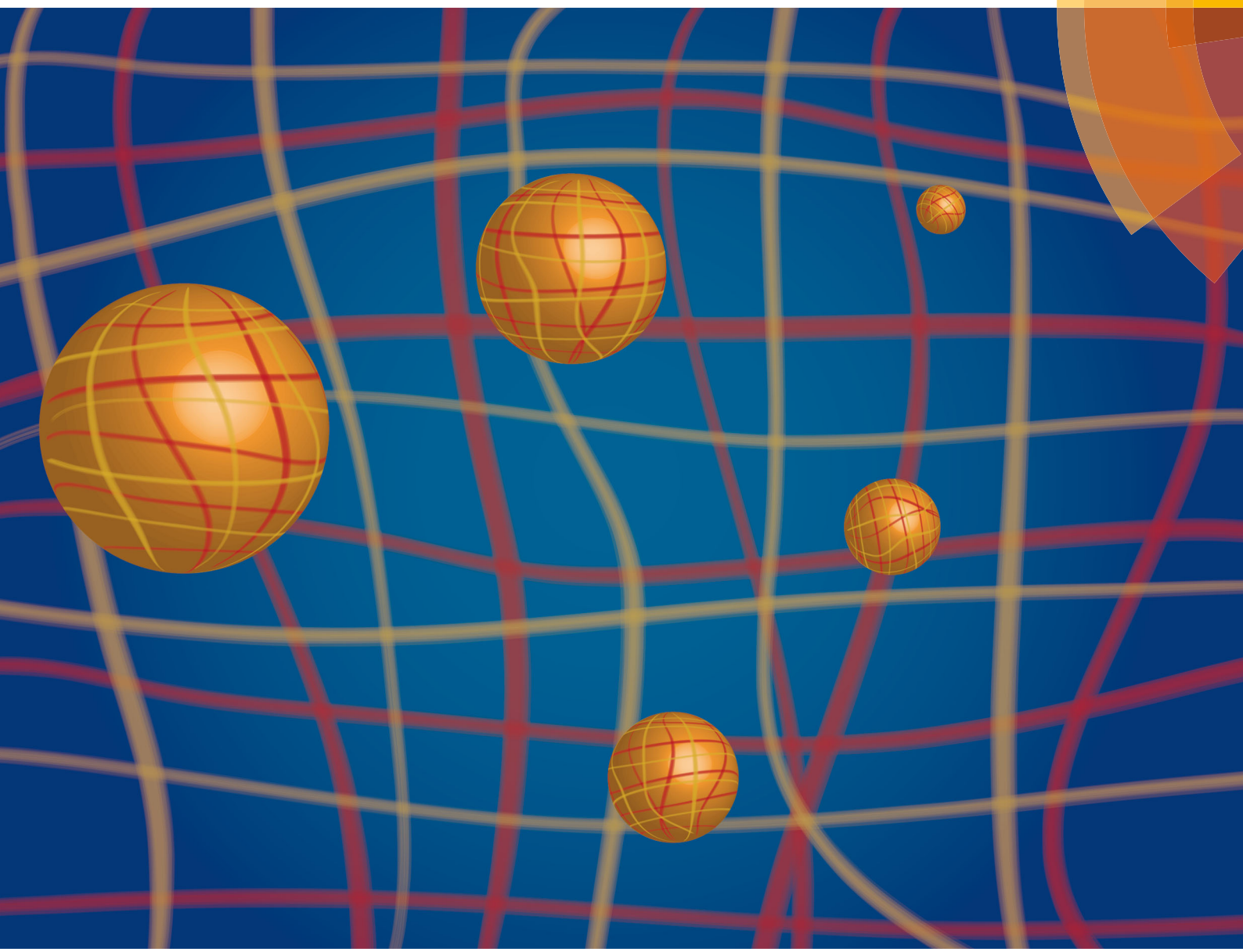

ISSN 1744-683X

ROYAL SOCIETY OF CHEMISTRY

PAPER
D. Appelhans, B. Voit *et al.*
Swelling behavior of bisensitive interpenetrating polymer networks for microfluidic applications

175 YEARS

Soft Matter

PAPER

View Article Online
View Journal | View Issue

Cite this: *Soft Matter*, 2016, 12, 5529

Swelling behavior of bisensitive interpenetrating polymer networks for microfluidic applications†

A. T. Krause,[a] S. Zschoche,[a] M. Rohn,[a] C. Hempel,[a] A. Richter,[b] D. Appelhans*[a] and B. Voit*[ac]

Received 24th March 2016,
Accepted 22nd April 2016

DOI: 10.1039/c6sm00720a

www.rsc.org/softmatter

Bisensitive interpenetrating polymer network (IPN) hydrogels of temperature sensitive *net*-poly(*N*-isopropylacrylamide) and pH sensitive *net*-poly(acrylic acid-*co*-acrylamide) for microfluidic applications were prepared *via* a sequential synthesis using free radical polymerization. The IPN indicated a suitable reversible alteration of swelling in response to the change in pH and temperature. The adequate change of the hydrogel volume is a basic requirement for microfluidic applications. Using the introduced correction factor *f*, it is possible to determine the cooperative diffusion coefficient (D_{coop}) of cylindrical samples at any aspect ratio. The determined cooperative diffusion coefficient allowed the evaluation of varying swelling processes of different network structures. The presence of the second sub-network of the IPN improved the swelling behaviour of the first sub-network compared to the individual networks.

Introduction

Hydrogels are polymeric networks containing a huge amount of water without being soluble. Stimuli sensitive hydrogels are able to undergo a reversible volume phase transition (VPT) and change their degree of swelling as a reaction to an external stimulus. Some popular stimuli are temperature,[1,2] pH value,[3] salt content,[4] alcohol concentration,[5] electrical field,[6] magnetic field,[7] light,[8] laser,[9] organic molecules like glucose[10] and antigens.[11] The many different possible stimuli lead to a large number of possible applications of responsive hydrogels, one of them is as active materials in microfluidics. This includes microfluidic sensors,[12] valves,[13] chemostats,[5] pumps,[14] and chemo-fluidic oscillators.[15] Furthermore there are possible applications in the field of drug-delivery-systems[16] or switchable membranes.[17] More detailed information about possible stimuli responsive hydrogel-based microfluidics can be found in the literature.[18,19]

The performance parameters for hydrogels in microfluidics are similar to conventional sensors: working range, measurement range, sensitivity, selectivity, reproducibility, long-term stability, response time and lifetime. In 2012 Richter *et al.* published a work reporting valves with a response time between milliseconds and several minutes depending on the applied characteristic length and stimuli.[20] Effective microfluidics needs further improved valve materials. One method to reduce the response time is the formation of a porous network.[21,22] In addition, miniaturization can help to reduce the response time.

In this context Beebe *et al.* worked on *net*-P(AA-*co*-HEMA) as a pH-sensitive actuator in microfluidic devices reacting to pH[23] and voltage[24] and realized a microfluidic flow sorter.[25] For that, they combined *net*-P(AA-*co*-HEMA) and *net*-P(DMAEMA-*co*-HEMA) in different channels of a T-junction. Enzyme loaded *net*-P(MAA-*graft*-TEGDMA) was used as a glucose sensitive valve material.[26]

The most used responsive hydrogel in microfluidics is *net*-PN*i*PAAm.[27] However, its potential when incorporated into an IPN for microfluidic applications is not yet investigated due to problems in achieving the required highly reproducible IPN materials with repeated stimuli response. Moreover their successful use in this application field demands (sub-)micrometer IPN shapes. A dual sensitivity of IPNs will further enhance their multiple use in microfluidic devices for complex work functions. It is desirable, for example, to generate valve materials with different degrees of permeability. So far, previous studies of acrylic acid and N*i*PAAm containing IPNs focused on the drug release behavior of IPNs, especially with pH- and temperature-response.[28–30]

This work is directed to establish a pH- and temperature-sensitive IPN as a hydrogel material for microfluidic applications with improved key parameters (*e.g.* mechanical stability and reproducible D_{coop} of defined hydrogel geometry). Basic parameters characterizing the performance of the hydrogels as sensor/actuator materials are investigated and improved performance for microfluidic actuators and sensors compared to classical hydrogels is demonstrated by the novel bisensitive IPNs.

[a] *Leibniz-Institut fuer Polymerforschung Dresden e.V., Hohe Strasse 6, 01069 Dresden, Germany. E-mail: voit@ipfdd.de*
[b] *Technische Universität Dresden, Chair of Polymeric Microsystems, 01062 Dresden, Germany*
[c] *Technische Universität Dresden, Faculty of Science, Organic Chemistry of Polymers, 01069 Dresden, Germany*

† Electronic supplementary information (ESI) available: Derivation of the correction factor *h*. See DOI: 10.1039/c6sm00720a

Tanaka kinetics

For being able to characterize the swelling speed of complex hydrogel materials with different dimensions and shapes we analyzed the swelling kinetics of our hydrogels. By that we aimed for the determination of the cooperative diffusion coefficient, which allows for predicting the swelling behavior of hydrogels independent of their size. This allows estimating the performance of hydrogels as sensor and actuator materials in microfluidics by analyzing few macroscopic samples. The basic equation is given by the heuristic model of Tanaka[31] for a spherical hydrogel particle:

$$\Delta a(t) = \Delta a_0 \cdot \left(\frac{6}{\pi^2}\right) \cdot \sum n^{-2} \cdot \exp\left(\frac{-n^2 t}{\tau}\right) \quad (1)$$

in which a is the characteristic size of a certain geometry, Δa_0 denotes the total increase of the characteristic size and τ is the characteristic swelling time. The characteristic length a means the smallest dimension of a cylindrical sample (half of the height for flat discs, radius for worm-like samples) or radius of a spherical sample. To simplify the equation, higher values of n can be neglected leading to the following equation:

$$\Delta a(t) = \Delta a \cdot \left(\frac{6}{\pi^2}\right) \cdot \mathrm{e}^{-\frac{t}{\tau}} \quad (2)$$

Transforming the equation and taking the logarithm result in,

$$\ln\left(\frac{\Delta a(t)}{\Delta a_0}\right) = -\frac{1}{\tau} \cdot t + \ln\left(\frac{6}{\pi^2}\right) \quad (3)$$

eqn (3) can be transformed into a classical linear equation:

$$\tau = -\frac{t}{\ln\left(\frac{\Delta a(t)}{\Delta a_0}\right)} + \ln\left(\frac{6}{\pi^2}\right) \quad (4)$$

Using the correlation between the characteristic swelling time and the cooperative diffusion coefficient, given by Tanaka, allows calculating the latter from the slope of the curve.

$$\tau = \frac{{a_\infty}^2}{\pi^2 D_{\mathrm{coop}}} \text{ or } D_{\mathrm{coop}} = \frac{{a_\infty}^2}{\pi^2 \tau} \quad (5)$$

a_∞ denotes the characteristic size at the end of swelling. It is not trivial to get appropriate values of D_{coop} from standard samples. The described geometries in the literature are only useful for extreme cases like very long or flat cylinders or spheres. Our investigated samples were of cylindrical shape with an aspect ratio (height divided by diameter) of around 1. This leads to the necessity of some kind of correction factor. Otherwise the calculated values for D_{coop} would be too small.[31] The approach is to assume a constant ratio of the cooperative diffusion coefficient and the volume specific surface A_V for all samples (eqn (6)). The correction factor f is defined to be the ratio of the cooperative diffusion coefficient of a cylindrical sample and a sphere or of the corresponding volume specific surfaces, respectively.

$$D_{\mathrm{coop,cylinder}} = \frac{A_{\mathrm{V,cylinder}}}{A_{\mathrm{V,sphere}}} D_{\mathrm{coop,sphere}} \quad (6)$$

$$D_{\mathrm{exp}} = f \cdot D_{\mathrm{coop}} \quad (7)$$

This leads to a general equation for f for long cylindrical (worm-like) samples as a result of the aspect ratio (height/diameter) AR > 1:

$$f_{h>d} = \frac{1 + 2\mathrm{AR}_{\mathrm{worm}}}{3\mathrm{AR}_{\mathrm{worm}}} \quad (8)$$

The general equation for f in the case of flat cylindrical (disc-like) samples with the aspect ratio (diameter/height) AR > 1 results in:

$$f_{d>h} = \frac{\mathrm{AR}_{\mathrm{cylinder}} + 2}{3\mathrm{AR}_{\mathrm{cylinder}}} \quad (9)$$

The correction factor equals 2/3, in the case of an infinite long (worm-like) cylinder (AR $\gg$ 1) and 1/3 in the case of an infinite flat (disc-like) cylinder (AR $\gg$ 1). Spherical samples (AR = 1) would exhibit a correction factor of 3/3.[32]

Thus, the correction factor f allows us to investigate cylindrical samples of arbitrary aspect ratios, correcting the calculated cooperative diffusion coefficients from the swelling kinetics and thus allows us to compare them with the results from dynamic light scattering (DLS) measurements[33,34] and with the results of other researchers.[31]

Materials and methods

Materials

N-Isopropylacrylamide (N*i*PAAm) (Acros Organics) was purified by recrystallization from *n*-hexane. *N*,*N*,*N*′,*N*′-Tetramethylethylenediamine (TMEDA) (Sigma Aldrich), sodium acrylate (NaAc) (Sigma Aldrich), acryl amide (AAm) (Fluka) and *N*,*N*′-methylenebisacrylamide (BIS) (Merck) were used without further purification. The initiator sodium peroxodisulfate (NaPS) (Riedel-de Haën) was used as a 0.84 molar aqueous solution (1.00 g in 5.0 mL of water). Commercially available buffer solutions (Certipur®, Merck) were used.

Synthesis of *net*-PN*i*PAAm

The *net*-PN*i*PAAm network was prepared by redox initiated free radical polymerization in water in an argon atmosphere. N*i*PAAm (937.5 mg, 8.3 mmol), BIS (12.8 mg, 0.083 mmol) and NaPS (49 μL of the stock solution) were dissolved in 6.56 g of deionized water. The solution was purged with nitrogen and cooled using an ice bath for 20 min. After initiating the polymerization with TMEDA (6 μL) the solution was filled into NMR tube like glass tubes of an inner diameter of around 4 mm and cooled at 15 °C for at least 3 hours in order to achieve homogeneous hydrogels.

The total monomer concentration was 12.5 wt%. 1 mol% cross-linker and 0.5 mol% initiator and accelerator with respect to the monomer were used.

Synthesis of *net*-P(AA-*co*-AAm)

net-P(AA-*co*-AAm) was synthesized by redox initiated free radical polymerization in water in an argon atmosphere.

NaAc (587.8 mg, 6.25 mmol), AAm (1331.3 mg, 18.75 mmol) and NaPS (238 μL of the stock solution) were dissolved in 18.07 g of deionized water. The solution was purged with nitrogen for 20 min. After initiating the polymerization with TMEDA (38 μL) the solution was filled into NMR tube like glass tubes of an inner diameter of around 4 mm and cooled at 15 °C for at least 3 hours.

The total monomer concentration was 9.6 wt%. 1 mol% cross-linker, 0.8 mol% initiator and 1.0 mol% accelerator, with respect to the monomer, were used.

Sequential synthesis of IPNs

Purified and swollen *net*-PN*i*PAAm cylinders of about 20 mm height were stored for at least 24 h in a 9.6 wt% monomer solution containing a 1 to 3 mole ratio of NaAc and AAm and 1 mol% cross-linker (Scheme 1). The amount of oxygen free monomer solutions was calculated to consistently result in an effective monomer concentration (lowered by the water of the pregels) of 9.1 wt%. The polymerization at 15 °C was started by adding 0.6 mol% NaPS and 0.7 mol% TMEDA and the polymerization period was 24 hours. Due to the significant difference in the degree of swelling the excess *net*-P(AA-*co*-AAm) hydrogel could be removed easily from the resulting IPN cylinder.

Following the IUPAC nomenclature the IPN is called *net*-poly(*N*-isopropylacrylamide)-*ipn*-[*net*-poly(acrylic acid-*co*-acrylamide)], abbreviated as *net*-PN*i*PAAm-*ipn*-[*net*-P(AA-*co*-AAm)].[35]

Purification of hydrogels

After the synthesis the hydrogels were removed out of the respective glass tubes (reaction vessel) and subsequently purified from polymerization residues by storing them in deionized water. After at least 24 h the water was changed. This was done 3 times. The IPN was first freed from overlaying *net*-P(AA-*co*-AAm) hydrogels. Then the *net*-P(AA-*co*-AAm) hydrogels were stored first in pH 4 buffer solution for at least 24 h and afterwards rinsed with water again to avoid the formation of cracks.

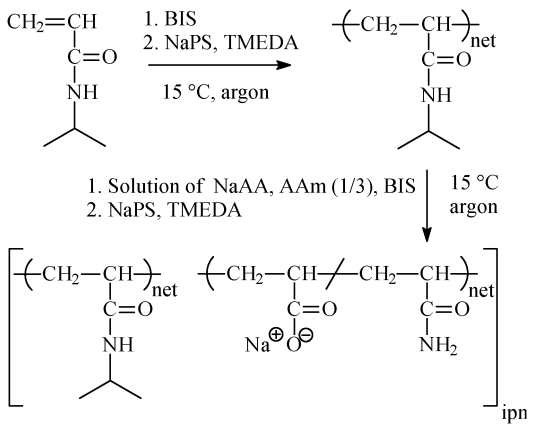

Scheme 1 Sequential synthesis of *net*-PN*i*PAAm-*ipn*-[*net*-P(AA-*co*-AAm)].

These freshly prepared samples were further used and preconditioned (*e.g.* pH-sensitive hydrogels: preconditioned for 24 h in pH 4 then added to the desired pH value; temperature-sensitive hydrogels: air-dried as the first step followed up by swelling in water at 50 °C; other combinations have also be studied) for the next experiments described below.

Measurement of the degree of swelling

To determine the degree of swelling, a small piece of a hydrogel sample at the equilibrium degree of swelling under particular pH (*e.g.* stepwise from pH 2 to pH 10) and temperature conditions (25 °C or 50 °C) was weighted and compared with its weight after freeze-drying. The weight degree of swelling is defined as the mass of the swollen hydrogel divided by the mass of the dried polymeric network:

$$Q_m = \frac{w_{swollen}}{w_{dry}} \quad (10)$$

We used the swelling ratio SR to describe the potential swelling capability of a hydrogel switching between two distinct stimulus conditions.

$$SR = \frac{Q_\infty}{Q_0} \triangleq \frac{Q_{End\ point}}{Q_{Starting\ point}} \quad (11)$$

Measurement of swelling kinetics

Cylindrical hydrogel test pieces with a height of around 2–6 mm and an aspect ratio of around 1 were cut from various synthesized cylinders using glass tubes with different inside diameters. Subsequently, the swelling was started by putting the sample at particular pH and temperature into a solution with a change in the pH-value (pH 4 to pH 9) or in temperature (50 °C to 25 °C). The swelling process was observed using a Leica S8APO microscope with a DFC295 camera (Leica) and a KL 1500 LCD (Schott) as a light source. Pictures were automatically taken using the Leica Application Suite Version 3.3.1. The evaluation was done manually. The swelling degree could be calculated from the diameter due to the isotropic swelling of hydrogels.

In every case just swelling was investigated. This prevents deswelling problems like the skin effect and the resulting non-equilibrium state, well known for *net*-PN*i*PAAm hydrogels. Samples must be optimal shaped and intact (crack- and air bubble-free). For this reason, *net*-PN*i*PAAm hydrogels were air-dried and reswollen in water at 50 °C before starting the swelling.

ATR-FTIR measurements

ATR spectra of freeze-dried samples were collected using a FTIR-spectrometer Vertex 80v (Bruker) equipped with a Golden Gate Diamond ATR unit (SPECAC) and a MCT-detector. The used spectroscopic range was 4000–600 cm^{-1}. The spectral resolution was 4 cm^{-1} and 100 scans were co-added for every spectrum. To compare ATR spectra properly, baseline correction and normalization were applied to all spectra. The combined methyl and methylene band area was used as reference in each spectrum.

The calibration curve was based on the normalized spectra of an adequate mixture of PN*i*PAAm, PAA and PAAm. Areas of

the amide II band of PN*i*PAAm at 1535 cm^{-1} were calculated and plotted as a concentration function.

Dynamic light scattering (DLS)

DLS measurements were carried out on an ALV-5000 compact goniometer system (ALV) equipped with a helium-neon laser (λ = 632.8 nm), coupled with an ALV photon correlator. All samples were measured at a scattering angle of $\theta = 90^\circ$ and a toluene bath was used for index matching and controlling the temperature at 25 °C. The time-averaged scattering intensities $\langle I\rangle_T$ and the time-averaged intensity correlation functions (ICF, $g_T^{(2)}(q,\tau) - 1$) were determined at 50 different sample positions selected by randomly rotating the cuvette before each run. The time for each run was 30 s. From the ICFs measured at each position, apparent diffusion coefficients D_A were estimated according to Shibayama:[36]

$$D_A = -\frac{1}{2q^2}\lim_{\tau\to 0}\frac{\partial}{\partial t}\ln\left(g_T^{(2)}(q,\tau) - 1\right) \quad (12)$$

Here, $q = (4\pi n/\lambda_0)\sin(\theta/2)$ is the scattering vector with θ being the scattering angle, λ_0 being the wavelength of the incident light in a vacuum, and n being the refractive index of the medium. For different sample positions, different values of D_A and the local scattering intensities $\langle I\rangle_T$ were obtained. The relationship between D_A and the cooperative diffusion coefficient, D_{coop}, is given by[37]

$$\frac{\langle I\rangle_T}{D_A} = \frac{2}{D_{coop}}\langle I\rangle_T - \frac{\langle I_F\rangle_T}{D_{coop}} \quad (13)$$

Plotting $\langle I\rangle_T/D_A$ *versus* $\langle I\rangle_T$, the data formed essentially a straight line, from whose slope and intercept the fluctuating component of the scattering intensity, $\langle I_F\rangle_T$, as well as D_{coop} was obtained.

All DLS measurements were performed on hydrogels under synthesis conditions and at RT and therefore directly investigated in the reaction vessel.

Results and discussion

Synthesis of IPNs

Using the synthetic approach presented in Scheme 1, IPNs of two independent sensitivities have been realized in cylindrical hydrogel geometries with various aspect ratios. Fig. 1 shows the relative swelling of *net*-PN*i*PAAm-*ipn*-[*net*-P(AA-*co*-AAm)] dependent on pH at room temperature (RT) and 50 °C compared to *net*-P(AA-*co*-AAm), measured at RT in dependence of pH. The IPN exhibits a significant change in the degree of swelling in response to the change in temperature and pH. The molar composition of the IPN, obtained from the synthesis conditions, is 54 mol% N*i*PAAm, 11.5 mol% AA and 34.5 mol% AAm. Due to the enormous swelling capabilities of polyelectrolyte hydrogels, only a low content of AA is needed in the IPN for a pronounced pH-sensitivity. ATR-FTIR measurements of IPNs allowed us to determine the acrylic acid units which are about 8% of all units within the IPN (ESI†).

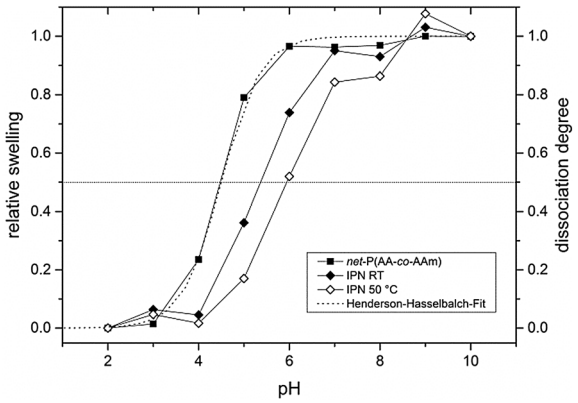

Fig. 1 pH-dependent swelling of *net*-P(AA-*co*-AAm) at RT with the Henderson–Hasselbalch-fit (dotted line, right ordinate) and of *net*-PN*i*PAAm-*ipn*-[*net*-P(AA-*co*-AAm)] at RT and 50 °C.

pK_a value of polyelectrolyte hydrogels

Fitting the pH-dependent swelling of *net*-P(AA-*co*-AAm) with the Henderson–Hasselbalch equation[38] leads to a pK_a value of 4.5 for *net*-P(AA-*co*-AAm) (Fig. 1). This is a simple method to characterize the pK_a of a polymer integrated in a hydrogel. The pK_a values of PAA in the literature vary from 4.5 to 6.4.[39,40] In the case of the IPN the curve of the *net*-P(AA-*co*-AAm) part exhibits a slight shift to higher pH. The pK_a value is about 5.4 (IPN, RT) or 6.1 (IPN, 50 °C). This effect can be explained by the sterical influence and partial non-responsiveness of the two networks within the IPN. In the case of increasing pH, the pH-sensitive subnetwork needs to extend the temperature-sensitive one, as it is not swelling on its own at higher pH values (Fig. 2). That is even more significant at temperatures above the volume phase transition temperature (VPTT) of *net*-PN*i*PAAm and results in the start of the swelling of the IPN at higher pH values (Fig. 1: ≥ pH 4). Another explanation is related to the interpolymer complexation between acrylic acid groups and *N*-isopropylacrylamide groups within the IPN. They form hydrogen bonds between each other which compete with polymer–water interactions.

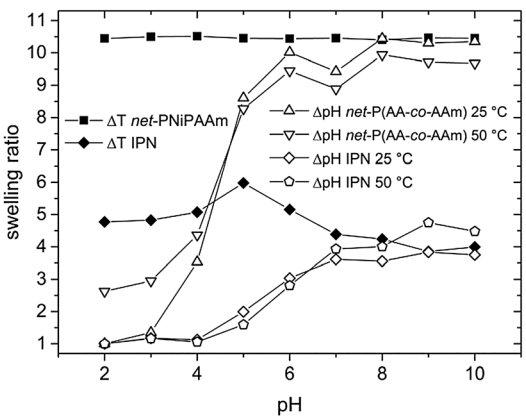

Fig. 2 Swelling ratio of different hydrogels at different pH values. Swelling degree of filled symbols calculated *via* $Q_{25°C}/Q_{50°C}$ and for hollow symbols *via* Q_{pHx}/Q_{pH2}.

Therefore, the degree of swelling of the IPN is lowered in comparison to *net*-P(AA-*co*-AAm) in the pH range of 2–4 where the necessary molecular acid groups occur.

Swelling ratio (SR)

The volume ratio between the swollen and deswollen state is an important value for the application of hydrogels as actuator/sensor materials in microfluidics. The SR can be easily derived by the swelling ratios of a sample at different states (stimuli). There are special demands on the degree of swelling in microfluidic applications as well as on the mechanical properties of the used hydrogels. A hydrogel doubling its size already exhibits a SR of 8 (2 cubed is 8), which therefore leads to an enormous demand in the volume change. A SR of 8 is challenging to realize for mechanical stable hydrogels but a good target value. The higher the SR is, the less the material is needed. A high SR allows the creation of fast switchable valves without increasing the microfluidic pressure of the system in the deswollen state too much. The SR of a hydrogel is an easily accessible and appropriate way to characterize the swelling performance of a hydrogel for microfluidic applications.

It is known from the literature that there is only a minor effect on VPTT of N*i*PAAm-based hydrogels by pH[41] (Fig. 2), while other stimuli (alcohol and salt) can distinctly affect the VPTT of *net*-PN*i*PAAm.[41,42] Polymeric hydrogel networks based on *net*-P(AA-*co*-AAm) exhibit a clear and significant sigmoidal pH-sensitive swelling (Fig. 2). The disparity between the swelling degrees of *net*-P(AA-*co*-AAm) at RT and 50 °C at low pH, shown in Fig. 2, is caused by the UCST-behavior of AA-containing hydrogels.[2] The IPN also exhibits a specific pH-sensitivity with a sigmoidal curve shape with increasing pH at room temperature and 50 °C. Comparing the pH-dependent SRs of the IPN and *net*-P(AA-*co*-AAm), a steric influence and non-responsiveness of net-PNIPAAm within the IPN are responsible for the lower pH dependent swelling ratio of the IPN than that of *net*-P(AA-*co*-AAm). Similar findings are present in the case of the T-dependent SR when comparing the IPN and *net*-PN*i*PAAm. Here, the presence of *net*-(PAA-*co*-AAm) suppresses the characteristics of *net*-PN*i*PAAm in the IPN. The subsequent application of IPN materials requires a defined environment to carry out a controllable and highly reproducible VPTT triggered by one selected stimulus.

Scheme 2 shows the swelling ratio of the investigated IPN selected from certain stimulus conditions in Fig. 2. The first step, starting at the deswollen state at 50 °C and pH 3, leads to an incompletely swollen state at 50 °C and pH 9 or 25 °C and pH 3 of the hydrogel. At this point one part of the IPN is collapsed and the other is swollen (*e.g.* for 25 °C and pH 3: swollen PN*i*PAAm and collapsed P(AA-*co*-AAm)). In the completely swollen state at 25 °C and pH 9 both parts of the IPN are swollen. Despite the lower SR of the IPN compared to the single components, each stimuli-responsive process within the swelling square presented in Scheme 2 shows a sufficient volume change as a result of an intensive optimization process. It is reasonable that the improvement of one stimulus in the swelling square will automatically affect the other stimulus. For example, in the case of a significantly improved temperature-sensitive SR

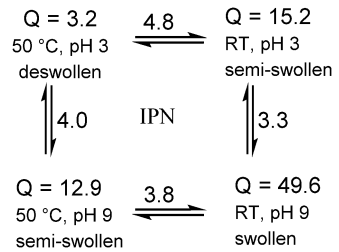

Scheme 2 Comparison of the equilibrium degrees of swelling of the IPN at deswollen, semi-swollen and swollen states and corresponding swelling ratios (on the arrows) of the corresponding swelling.

in the IPN, the capability of the pH-sensitive network will be decreased automatically. This is consequently governed by the product of two consecutive swelling changes which is equal to the value of the diagonal swelling ratio mentioned below.

For a successful use of the IPN in microfluidics it is a necessary prerequisite to establish IPNs with a highly reproducible change in the degree of swelling when applying different pathways (semi-swollen-states in Scheme 2) finally to achieve the completely swollen state. For this purpose the diagonal swelling ratio (top left to bottom right, Scheme 2) helps to provide the chance of good absolute swelling ratios for both steps (deswollen to semi-swollen and semi-swollen to swollen).

For the investigated IPN the diagonal swelling ratio is about 15.5. There are two possibilities to improve this value. The first is simply by increasing the maximum degree of swelling in the completely swollen state. The problem of diminishing mechanical toughness limits this possibility. The smarter way is to decrease the degree of swelling in the deswollen state since this will affect less the mechanical properties.

Swelling kinetics

The aim of analyzing the swelling kinetics is to determine the cooperative diffusion coefficient D_{coop} for different swelling processes of a hydrogel. D_{coop} is a parameter independent of geometry and size for different hydrogels and shall allow forecasting the swelling progress of an identical hydrogel with arbitrary geometry and size. D_{coop} can be used to describe the swelling kinetics of different hydrogel networks, assuming that the cooperative mobility of the subchains within a network is the rate determining step of the whole swelling process. Generally, D_{coop} has to be slower than the diffusion of the stimulus into the hydrogel. The thermal transfer is around 10^{-3} cm^2 s^{-1} and the diffusion of pH is 10^{-5} cm^2 s^{-1}. Common values of D_{coop} for subchains within a network are 10^{-6} down to 10^{-7} cm^2 s^{-1}.[43] Thus, the improvement of swelling speed by modifying D_{coop} is limited and needs to be supplemented by taking geometry and size into consideration.

A direct comparison of swelling times of different hydrogels is not suitable because of the differences in the sample size and the aspect ratio, presented in Table 1. Fig. 3 shows the temperature dependent swelling of three IPN samples possessing different aspect ratios. Therefore the swelling data have to be evaluated by using the swelling kinetics model of Tanaka (eqn (4)) and the

Table 1 Temperature-dependent swelling of flat cylindrical IPN samples with different aspect ratios

IPN	a [mm]	AR	τ [s]	f	D_{exp} [cm^2 s^{-1}]	D_{exp}/f [cm^2 s^{-1}]
Sample 1	1.17	2.78	2780	0.573	5.02×10^{-7}	8.76×10^{-7}
Sample 2	1.63	2.00	4528	0.667	5.97×10^{-7}	8.95×10^{-7}
Sample 3	2.31	1.37	7662	0.821	7.08×10^{-7}	8.62×10^{-7}

a = characteristic length, AR = aspect ratio, τ = characteristic swelling time, f = shape correction factor, and D_{exp} = experimental cooperative diffusion coefficient.

appropriate form correction factor f (eqn (7)). Fig. 4 exemplarily shows the kinetic plot by Tanaka of the time dependent swelling of *net*-PN*i*PAAm-*ipn*-[*net*-P(AA-*co*-AAm)] samples (Fig. 3). Only the integration of the correction factor f in the kinetic model of Tanaka yet allows the comparison of the form-corrected cooperative diffusion constants (D_{exp}/f) for the different IPN samples (Table 1). The normal cooperative diffusion constant calculated from the kinetic plot by Tanaka (Fig. 4) gives different values for the different IPN samples (Table 1). The correction factor f adjusts the different aspect ratios of the samples and results in the desired and comparable D_{exp}/f summarized in Table 1. The resultant data of the corrected value of D_{exp} exhibit a small standard deviation ($D_{exp}/f = 8.78(\pm 0.17) \times 10^{-7}$ cm^2 s^{-1}). This implies that the use of the correction factor f enables us to compare the swelling kinetics of differently sized examples of the same shape.

Swelling characteristics dependent on stimuli and networks

Table 2 shows the compilation of investigated hydrogels and their cooperative diffusion coefficients. All swelling kinetics were carried out at least 3 times with different cylindrical samples each.

Applying an imperfect network for the determination of D_{coop}, *e.g.* in the case of placing *net*-PN*i*PAAm samples directly from RT into an aqueous solution of 50 °C (ΔT), the D_{coop} and the standard deviation for this *net*-PN*i*PAAm samples were quite high with a result of $D_{coop} = 14.7 \pm 3.89 \times 10^{-7}$ cm^2 s^{-1}. Under these conditions *net*-PN*i*PAAm hydrogels suffer small

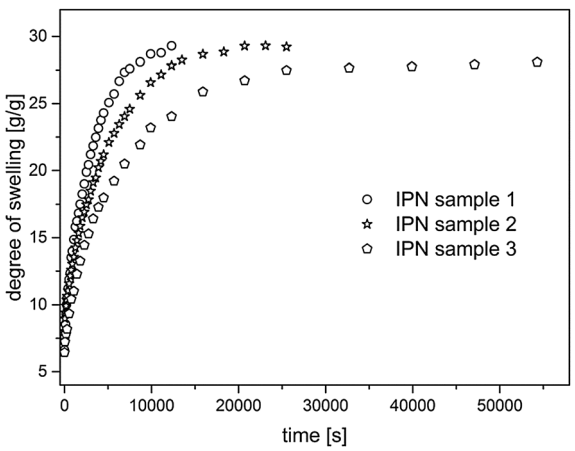

Fig. 3 Time dependent swelling of cylindric samples of IPNs, possessing different aspect ratios, with a change in temperature from 50 °C to 25 °C at pH 4.

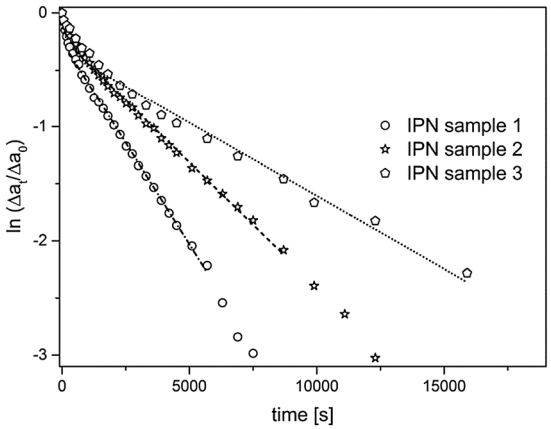

Fig. 4 Kinetic plot by Tanaka, using eqn (4), for temperature-dependent swelling of IPN samples at pH 4.

cracks caused by the drastic VPT. These cracks only provide a reduced effective characteristic length for the application of the corresponding equation (eqn (9)). This subsequently results in an irregular high D_{coop} value and an increased standard deviation. In contrast to this, IPNs do not show the formation of cracks when applying the same experimental conditions as applied for *net*-PN*i*PAAm or *net*-P(AA-*co*-AAm) samples. From these first experiments one can conclude that IPNs show the desirable improved mechanical stability for their application as sensor/actuator materials in microfluidics. Furthermore, the investigated IPN does not show any skin effect compared to *net*-PN*i*PAAm.[44]

We determined D_{coop} for a regular (see chapter: Measurement of swelling kinetics) *net*-PN*i*PAAm to be 3.8×10^{-7} cm^2 s^{-1} (Table 2) matching the literature value of 3.2×10^{-7} cm^2 s^{-1}.[31]

The D_{coop} values for the pH-sensitive *net*-P(AA-*co*-AAm), determined at ΔpH (Table 2), are larger than those for the temperature-sensitive *net*-PN*i*PAAm, determined at ΔT. This fits to the assumption that polyelectrolyte-based hydrogels swell faster than others due to their charges.[44]

Furthermore the temperature-response of the IPN, determined by the combination of ΔT and pH 4, is faster than the pregel *net*-PN*i*PAAm under ΔT conditions. This effect is even bigger when observing the temperature-dependent swelling of the IPN at ΔT and pH 9. This is caused by the additional swelling of pH sensitive part of the IPN. Overall the IPNs possess a higher D_{coop} as found for the IPN with ΔT at pH 4. The acceleration of IPN swelling is dependent on the pH value, as the pH-dependent swelling is correlated with the degree of dissociation. Thus, higher dissociation degrees at higher pH values ($\geq$pH 5) lead to an accelerated swelling of the IPN and a higher D_{coop}. This can be explained by the increased osmotic pressure of the deprotonated acid groups.

In contrast, the pH-response of the IPN at RT is as fast as the corresponding *net*-P(AA-*co*-AAm). In this case the 2nd network PN*i*PAAm is not stretching the stimulated one and cannot accelerate the swelling. In conclusion this implies that both subnetworks mutually affect their swelling depending on their own tendency to swell according to the stimulus conditions.

Moreover, there is good congruence between the D_{coop} values investigated by DLS and swelling kinetics (Table 2) for

Table 2 Diffusion coefficient dependent on swelling processes and networks

Hydrogel	Swelling process	Stimulus	D_{DLS} ($cm^2\ s^{-1}$)	D_{coop} ($cm^2\ s^{-1}$)
net-PNiPAAm	50 °C to 25 °C	ΔT	4.6×10^{-7}	$3.8 \pm 0.23 \times 10^{-7}$
IPN	50 °C to 25 °C; at pH 4	ΔT		$8.8 \pm 0.14 \times 10^{-7}$
IPN	50 °C to 25 °C; at pH 9	ΔT		$20.0 \pm 0.49 \times 10^{-7}$
net-P(AA-*co*-AAm)	pH 4 to pH 9; at 25 °C	ΔpH	10.6×10^{-7}	$9.4 \pm 0.42 \times 10^{-7}$
IPN	pH 4 to pH 9; at 25 °C	ΔpH		$9.4 \pm 0.19 \times 10^{-7}$

both *net*-PN*i*PAAm and *net*-P(AA-*co*-AAm). DLS requires transparent, dust- and bubble-free samples which are difficult to achieve. In addition DLS is hard to execute at swelling degrees other than those resulting directly from the synthesis. Additionally, preparing appropriate IPN samples for DLS using the sequential synthesis was not possible.

Overall, the swelling kinetics is more suitable to characterize the swelling behavior of complex hydrogels such as IPNs for microfluidics.

Prediction of swelling time

The characteristic swelling time for hydrogel samples of any size can be calculated using determined D_{coop} and the Tanaka equation (eqn (5)). The only limitation is the sample geometry. Spherical and cylindrical samples can be described using this approach. To prove this, cylindrical shapes have been used for the prediction model of swelling. Fig. 5 shows the characteristic swelling time against the characteristic length for the temperature-dependent swelling of the cylindrical IPN.

The swelling time of any sample size can be predicted using the slope of a best fit straight line. This leads to a characteristic swelling time of around 10 seconds at sizes of around 100 μm. These size dimensions are usually used in microfluidics in the case of spherical samples without any constraints.[20]

The dependency between τ and D_{coop} (eqn (5)), given by Tanaka[31], allows the characterization of hydrogels of convenient size and predicting their performance as actuator and sensor materials in microfluidic dimensions. The effect of constrained diffusion and convection by covered parts of the hydrogel or even covalently bonded surfaces is not properly considered by the use of the correction factor *f*. But it could be addressed by adequately modifying the correction factor *f*.

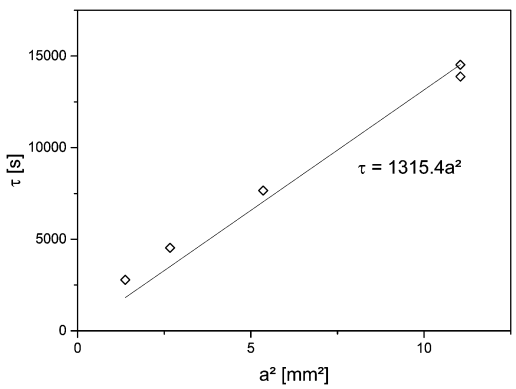

Fig. 5 Characteristic swelling time against characteristic length squared for temperature-sensitive swelling of cylindrical IPNs.

Conclusions

A novel bisensitive IPN, designed for microfluidic actuators and sensors, is presented. The created double network *net*-PN*i*PAAm-*ipn*-[*net*-P(AA-*co*-AAm)], consisting of a total monomer ratio of N*i*PAAm/AA/AAm of about 68/8/24, exhibits a stimuli-dependent VPTT to two different stimuli, namely temperature and pH. This makes it an interesting material for chemical transistors and valves in microsystems. The IPN was characterized by its swelling ratio SR, which is an easily accessible parameter to characterize the swelling capability of hydrogels for microfluidics. The diagonal swelling ratio of IPNs is a suitable value to characterize them. The reduced swelling capability due to the 2nd network makes IPNs even more suitable for the application in microfluidics because of the correlated further improvement of the mechanical properties. The swelling ratios of the investigated IPN are between 3 and 5 which are suitable for microfluidic applications, but they can be further improved based on tailored synthesis conditions, composition of networks and network ratios to reach consistently values above 4.

Using the introduced correction factor *f*, the modified Tanaka[31] equation is able to determine the cooperative diffusion coefficients of cylindrical IPN samples at any aspect ratio. By investigating the characteristic swelling time of differently sized samples, the swelling time (switching on/off) of valves can be estimated. This results, for example, in a swelling time of about 13 seconds for the temperature-dependent swelling of IPNs with a characteristic length of 100 μm at pH 4. This allows us to characterize the swelling kinetics and to predict the swelling behavior of hydrogels at a μm scale.

Additionally, the measured D_{coop} allows the evaluation of swelling processes of different network structures. The two IPN-forming network parts interfere with each other. The temperature swelling of IPNs is clearly accelerated, due to the faster swelling of the *net*-P(AA-*co*-AAm) sub-network, especially at higher dissociation degrees.

Furthermore, the mechanical stability of IPNs is superior to that of classical hydrogels, as they do not crack under harsh treatment. This can be easily detected *via* the enlarged standard deviation of D_{coop} or just the shortened swelling time. The observed high reproducibility and mechanical stability, even under a drastically change of stimuli, make IPNs appropriate for reusable devices in microfluidics.

Acknowledgements

This work is funded by the German Research Foundation (DFG) within the Research Training Group GRK 1865/1 "Hydrogel-Based Microsystems". Mikhail Malanin is gratefully acknowledged for carrying out the ATR-TFIR measurements.

References

1 R. Pelton, *Adv. Colloid Interface Sci.*, 2000, **85**, 1–33.
2 B. V. Slaughter, A. T. Blanchard, K. F. Maass and N. A. Peppas, *J. Appl. Polym. Sci.*, 2015, **132**, 42076.
3 A. Richter, G. Paschew, S. Klatt, J. Lienig, K.-F. Arndt and H.-J. P. Adler, *Sensors*, 2008, **8**, 561–581.
4 M. Panayiotou and R. Freitag, *Polymer*, 2005, **46**, 6777–6785.
5 A. Richter, A. Türke and A. Pich, *Adv. Mater.*, 2007, **19**, 1109–1112.
6 T. Tanaka, I. Nishio, S.-T. Sun and S. Ueno-Nishio, *Science*, 1982, **218**, 467–469.
7 R. Koseva, I. Mönch, J. Schumann, K.-F. Arndt and O. G. Schmidt, *Thin Solid Films*, 2010, **518**, 4847–4851.
8 A. Suzuki and T. Tanaka, *Nature*, 1990, **346**, 345–347.
9 S. R. Sershen, G. A. Mensing, M. Ng, N. J. Halas, D. J. Beebe and J. L. West, *Adv. Mater.*, 2005, **17**, 1366–1368.
10 T. Ye, S. Yan, Y. Hu, L. Ding and W. Wu, *Polym. Chem.*, 2013, **5**, 186.
11 T. Miyata, N. Asami and T. Uragami, *Nature*, 1999, **399**, 766–769.
12 X. Liu, X. Zhang, J. Cong, J. Xu and K. Chen, *Sens. Actuators, B*, 2003, **96**, 468–472.
13 Y. Osada and Y. Takeuchi, *J. Polym. Sci., Polym. Lett. Ed.*, 1981, **19**, 303–308.
14 A. Richter, C. Klenke and K.-F. Arndt, *Macromol. Symp.*, 2004, **210**, 377–384.
15 G. Paschew, J. Schreiter, A. Voigt, C. Pini, J. P. Chávez, M. Allerdißen, U. Marschner, S. Siegmund, R. Schüffny, F. Jülicher and A. Richter, *Adv. Mater. Technol.*, 2016, **1**, 1600005.
16 T. R. Hoare and D. S. Kohane, *Polymer*, 2008, **49**, 1993–2007.
17 K. Sumaru, K. Ohi, T. Takagi, T. Kanamori and T. Shinbo, *Langmuir*, 2006, **22**, 4353–4356.
18 P. Schattling, F. D. Jochum and P. Theato, *Polym. Chem.*, 2014, **5**, 25–36.
19 N. A. Peppas, B. V. Slaughter and M. A. Kanzelberger, *Polymer Science: A Comprehensive Reference*, Elsevier, 2012, ch. 20, vol. 9, pp. 385–395.
20 R. Greiner, M. Allerdissen, A. Voigt and A. Richter, *Lab Chip*, 2012, **12**, 5034.
21 W.-F. Lee and H.-C. Lu, *J. Appl. Polym. Sci.*, 2013, **127**, 3663–3672.
22 V. Schulz, S. Zschoche, H. P. Zhang, B. Voit and G. Gerlach, *Procedia Eng.*, 2011, **25**, 1141–1144.
23 R. H. Liu, Q. Yu and D. J. Beebe, *J. Microelectromech. Syst.*, 2002, **11**, 45–53.
24 M. J. Bassetti and D. J. Beebe, *Micro Total Analysis Systems*, Kluwer Academic Publishers, Nara Japan, 2002.
25 D. J. Beebe, J. S. Moore, J. M. Bauer, Q. Yu, R. H. Liu, C. Devadoss and B.-H. Jo, *Nature*, 2000, **404**, 588–590.
26 X. Cao, S. Lai and L. James Lee, *Biomed. Microdevices*, 2001, **3**, 109–118.
27 M. E. Harmon, M. Tang and C. W. Frank, *Polymer*, 2003, **44**, 4547–4556.
28 Z. Xing, C. Wang, J. Yan, L. Zhang, L. Li and L. Zha, *Soft Matter*, 2011, **7**, 7992.
29 W.-F. Lee and H.-C. Lu, *J. Appl. Polym. Sci.*, 2013, **127**, 3663–3672.
30 S. Chen, M. Liu, S. Jin and Y. Chen, *Polym. Bull.*, 2014, **71**, 719–734.
31 T. Tanaka and D. J. Fillmore, *J. Chem. Phys.*, 1979, **70**, 1214.
32 Y. Li and T. Tanaka, *J. Chem. Phys.*, 1990, **92**, 1365.
33 M. Shibayama, Y. Shirotani and Y. Shiwa, *J. Chem. Phys.*, 2000, **112**, 442.
34 H. Furukawa, K. Horie, R. Nozaki and M. Okada, *Phys. Rev. E: Stat., Nonlinear, Soft Matter Phys.*, 2003, **68**, 031406.
35 R. C. Hiorns, R. J. Boucher, R. Duhlev, K.-H. Hellwich, P. Hodge, A. D. Jenkins, R. G. Jones, J. Kahovec, G. Moad, C. K. Ober, D. W. Smith, R. F. T. Stepto, J.-P. Vairon and J. Vohlídal, *Pure Appl. Chem.*, 2012, **84**, 2167.
36 M. Shibayama, *Macromol. Chem. Phys.*, 1998, **199**, 1–30.
37 J. G. H. Joosten, E. T. F. Geladé and P. N. Pusey, *Phys. Rev. A: At., Mol., Opt. Phys.*, 1990, **42**, 2161–2175.
38 P. Muller, *Pure Appl. Chem.*, 1994, **66**, 1077.
39 K. F. Tjipangandjara and P. Somasundaran, *Adv. Powder Technol.*, 1992, **3**, 119–127.
40 J. Choi and M. F. Rubner, *Macromolecules*, 2005, **38**, 116–124.
41 X. Liu, *Biomaterials*, 2004, **25**, 5659–5666.
42 A. Hüther, X. Xu and G. Maurer, *Fluid Phase Equilib.*, 2004, **219**, 231–244.
43 A. Richter, G. Paschew, S. Klatt, J. Lienig, K.-F. Arndt and H.-J. P. Adler, *Sensors*, 2008, **8**, 561–581.
44 A. Richter, S. Howitz, D. Kuckling and K.-F. Arndt, *Sens. Actuators, B*, 2004, **99**, 451–458.

